RSC Advances

ROYAL SOCIETY OF CHEMISTRY

www.rsc.org/advances

RSC Advances

RSCPublishing

COMMUNICATION

Genetically encoded phenyl azide photochemistry drives positive and negative functional modulation of a red fluorescent protein

Cite this: DOI: 10.1039/x0xx00000x

Received 00th January 2012,
Accepted 00th January 2012

DOI: 10.1039/x0xx00000x

www.rsc.org/

Samuel C. Reddington[a,$], Sarunas Driezis[a,$], Andrew M. Hartley[a,$], Peter D. Watson[a] Pierre J. Rizkallah[b] & D. Dafydd Jones[a]*.

The photochemical properties of phenyl azide have been exploited to modulate the function of a red autofluorescent protein, mCherry. Using genetic code reprogramming, phenyl azide chemistry has been introduced at functionally strategic positions in mCherry leading to deactivation, activation or enhancement upon UV irradiation.

Optical control of biological processes whereby light is used to modulate inherent protein function is fast becoming an important tool in the biosciences as a means to precisely control protein activity with high temporal and spatial resolution not achievable through classical transcriptional control [1-3]. Existing approaches to genetically encode protein photocontrol, known as optogenetics, generally utilise versions of natural light sensing proteins that detect and respond to light through the use of non-proteinaceous cofactors (e.g. retinal and flavins). The main drawback is the requirement for whole protein domains (e.g. LOV domains [4] or membrane bound opsins [2]) to encode the light-responsive properties. An alternative approach is to use photoreactive chemical groups that can be programmed directly into a protein through the use of non-canonical amino acids (ncAAs) [5]. One such ncAA, *p*-azido-phenylalanine (azF; Fig 1a), is particularly useful as it has a relatively small side-chain compared to other ncAAs (N_3 at the *para* position instead of OH in the natural amino acid tyrosine) and can easily be photoconverted to a highly reactive nitrene radical (Fig 1a) [6, 7]. Subsequent products of the various nitrene reaction pathways can be used to alter protein structure and thus control function [8].

Autofluorescent proteins are unique in nature in that they absorb and emit light in the visible range without the requirement of cofactors [9, 10]. Contiguous amino acids within the core of the protein covalently rearrange in the presence of O_2 to form an extended conjugated π system that acts as a chromophore. Photoresponsive versions of autofluorescent proteins are critical to modern super-resolution microscopy [11]. The two main classes of autofluorescent proteins are the green [10] (primarily derived from the classical *Aequorea victoria* GFP) and red [9] (primarily derived from the oligomeric Discosoma sp. DsRED) versions. While the two protein classes share a common β-can structure, their sequence identities are low with distinct chromophore structures, maturation and environment; all these factors contribute towards the significant differences in fluorescence between these autofluorescent protein. Thus, useful mutations cannot always be simply transferred to the other. Red autofluorescent proteins are becoming the preferred option in cell imaging due to their lower excitation wavelength energy and reduced inherent cellular fluorescence background. While previous efforts have highlighted how ncAAs [12], including azF [13, 14], can influence the properties of GFPs, little is known about their potential impact and use with respect to red versions. Here we address this using the widely used DsRed variant mCherry [15] and show by replacing single pre-selected residues with azF how function can be either positively or negatively regulated by UV irradiation, both *in vitro* and *in vivo*.

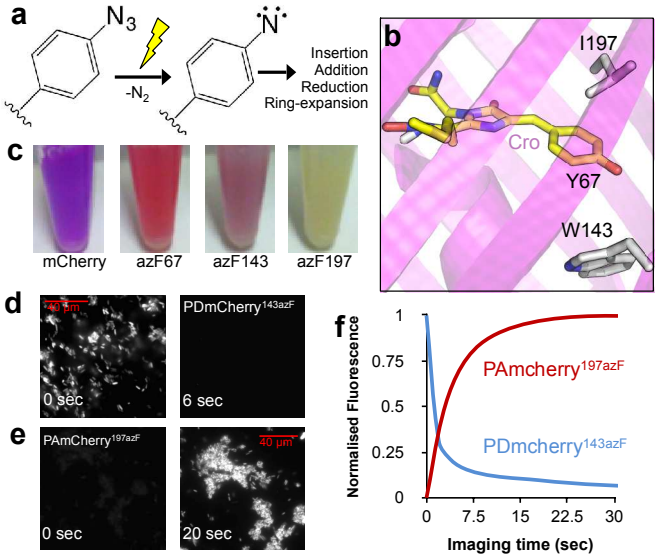

Fig 1. Incorporation of phenyl azide chemistry into mCherry. (a) Side chain and photochemical properties of *p*-azido-L-phenylalanine (azF). (b) Selected residues in mCherry where azF incorporation instilled photochemical control on the protein. (c) The effect of azF incorporation at the selected residues in mCherry on the transmissive colour. (d) Photodeactivation of PDmCherry^{143azF} and (e)

photoactivation of PAmCherry^{197azF} in live cells after UV irradiation at 350 nm. (f) Change in live cell fluorescence over time for PDmCherry^{143azF} and PAmCherry^{197azF} on irradiation at 350 nm. Live cell imaging was performed using widefield microscopy.

Based on analysis of the mCherry structure [PDB 2H5Q [16]], residues in and around the chromophore were selected for replacement with azF (Fig 1b and Fig S1). Of the twelve different mutants generated, ten were produced as soluble protein, suggesting incorporation of azF within the protein core did not impact protein folding (Table S1). All but two of the soluble variants had a measureable fluorescent signal before and/or after UV irradiation, suggesting that azF is functionally tolerated within the core of the protein. On UV irradiation, fluorescence changes varied depending on the placement of azF and included decreases, increases and/or shifts in λ_{EX} and λ_{EM} (Table S1). While mCherry itself has a degree of sensitivity to UV light (Table S1 and Fig S2), most of the photoresponsive azF mutants displayed a significantly greater magnitude of change. Three variants (Y67azF, W143azF and I197azF; Fig 1b) exhibited the largest fold change in fluorescence and were selected for further characterisation.

Replacement of W143 with azF (termed PDmCherry^{143azF}, where PD refers to photodeactivation) generated a highly fluorescent protein in its dark state (pre-irradiation) that was responsive to UV light. Prior to irradiation, widefield microscopy of live *E. coli* cells indicated that PDmCherry^{143azF} was relatively stable to photobleaching with a $t_{1/2}$ of 76 sec at 555 nm under typical imaging conditions for mCherry. The spectral peaks were slightly blue shifted (2-5 nm) compared to mCherry and it had a 20% lower quantum yield (Φ) and ~50% lower molar extinction coefficient (ε) (Table 1). PDmCherry^{143azF} was very sensitive to UV light (Fig 1d), with live cell imaging revealing irradiation at 350 nm rapidly decreased observed fluorescence beyond the level inherent to mCherry (Fig S2) with a $t_{1/2}$ of 10 sec. Detailed *in vitro* analysis confirmed these findings with PDmCherry^{143azF} converting to a form with low fluorescence (Fig 2a and Table 1). The absorbance spectrum indicated that photolysed protein still retained an entity that acts as a chromophore (λ_{max} 582 nm), albeit with a slightly lower extinction coefficient (Fig 2b).

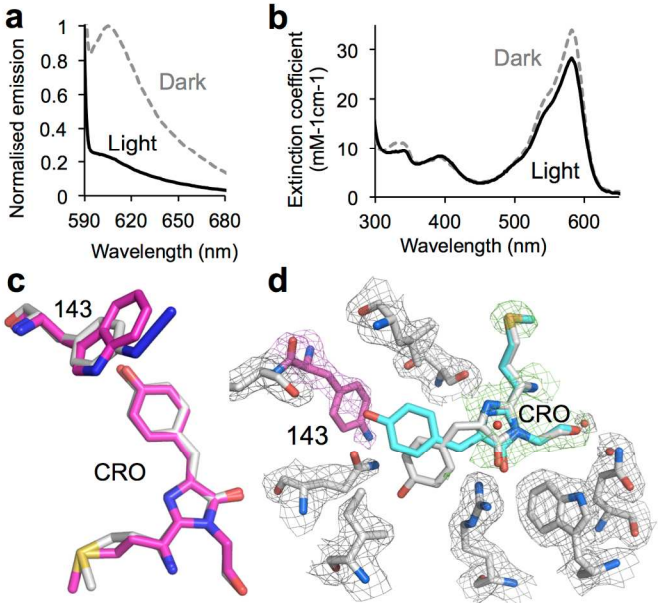

Fig 2. Photodeactivation properties of PDmCherry^{143azF}. (a) Fluorescence emission spectra (on excitation at 584 nm) and (b) corresponding absorbance spectra of protein before (Dark; grey dashed line) and after (Light; black line) UV irradiation (60 min). (c) Crystal structure of the dark state PDmCherry^{143azF} (carbons coloured grey) compared to mCherry structure (carbons coloured magenta) highlighting the chromophore (CRO) and residue 143. (d) The structure of the light state PDmCherry^{143azF} with the electron density maps of CRO (grey/cyan), residue 143 (magenta) together with surrounding residues (grey) shown. Potential conformations for CRO are modelled in.

To investigate the potential mechanism of action, the crystal structures of PDmCherry^{143azF} resolved to 1.7 Å (dark; PDB code 4ZIN) and 2.0 Å (light; PDB code 4ZIO) were determined (see Supporting Information for details). The structure of the dark state revealed that the variant has an essentially identical structure to mCherry with both the chromophore and residues at 143 occupying similar positions and planes (Fig 2c). The packing around the chromophore was also very similar (Fig S3). Thus, inserting a phenyl azide moiety into the core of the protein did not significantly disrupt structure. However, the presence of the azide group with its inherent resonance structures close to the chromophore may be influencing the latter's electronic properties.

Table 1. Spectral properties of purified mCherry^{azF} variants.

Variant	λ_{max} (nm)	λ_{ex} (nm)	λ_{em} (nm)	State	ε ($M^{-1}cm^{-1}$)	Φ	Brightness $M^{-1}cm^{-1}$	Fold change[a]
PDmCherry W143azF	582	584	608	Dark	34,000	0.18	6,120	5.1
				UV[b]	25,800	0.06	1,548	
PAmCherry I197azF	584	587	610	Dark	<1,000	ND[c]	-	≥14.1
				UV[b]	11,600	0.05	580	
mCherry[d]	587	587	610	-	72,000	0.22	15,840	-

[a] Fold change in fluorescence of variants was calculated from *in vitro* fluorescence spectra before and after photolysis. [b] Irradiated using a 5W handheld lamp. [c] ND = not determined. The quantum yield of PAmCherry^{I197azF} before photolysis was too low to be determined as protein absorbance (ε) was too low. [d] from N. C. Shaner, et al, *Nat Biotech*, 2004, 22, 1567-1572.

Residue 143 lies close to the chromophore in mCherry (and the W143azF variant; Fig 2c), occupying an equivalent position to Y/F145 in GFP, but both the backbone and the side chain placements differ significantly between the two (Fig S4). Replacement of F145 in superfolder GFP (sfGFP[17]) with azF also led to loss of fluorescence on irradiation [14] but by a different mechanism; the phenyl nitrene forms a crosslink to the chromophore so restricting chromophore mobility and reducing the extended conjugated double bond system. In contrast, the structure of irradiated PDmCherry^{143azF} strongly suggests increased chromophore mobility is causing loss of fluorescence (Fig 2d) with little change to the chromophore structure (Fig 2b). The electron density for the irradiated form was generally poor over the chromophore region and residue 143, with no electron density observed for the p-hydroxybenzylidene chromophore moiety (Fig 2d). The most likely explanation is the absence of a single defined conformation of the chromophore in the crystal, which suggests conformational flux of the chromophore upon UV irradiation of PDmCherry^{143azF}. Isomerism and bond angle changes involving the chromophore are known to influence fluorescence [11]. Indeed, the hydroxybenzylidene can be modeled to both the *cis* and *trans*

conformation without steric problems or overlap with observed electron density (Fig 2d). The limited electron density observed for residue 143 suggests a single atom protrusion at the *para* position, which we have tentatively assigned as the phenyl amine product of azF photolysis (Fig 2d). The side chain of residue 143 points away from the chromophore, with the likely position of the nitrene radical being too far away (5.5–6 Å) to form a crosslink with the chromophore (Fig 2d). The similar absorbance spectra for both dark and light forms of PDmCherry^{143azF} suggest that the chemical structure is not significantly perturbed on irradiation. Otherwise, the structures of the dark and light states are very similar (Fig S3) highlighting the crucial role relatively small structural changes instigated by azF photochemistry have on modulating fluorescent protein function and local dynamics.

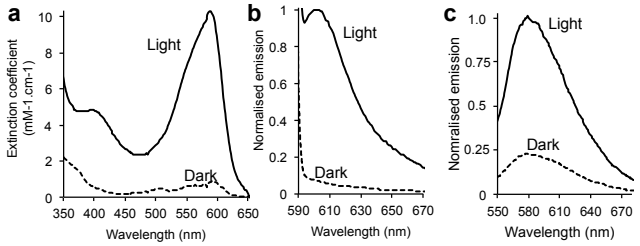

Fig 3. Photoactivating mCherry azF variants. (a) Absorbance and (b) fluorescence emission (excited at 587 nm) spectra of PAmCherry^{197azF} before (Dark) and after (Light) UV irradiation. (c) The emission spectra of PEmCherry^{67azF} on excitation at 541 nm before (Dark) and after (Light) UV irradiation.

Replacement of I197 with azF resulted in the production of a non-fluorescent protein (termed PAmCherry^{197azF}, where PA refers to photoactivation) with little inherent colour (Fig 1c), cellular fluorescence (Fig 1d) or absorbance (Fig 3a). Neither the Φ nor ε for the non-irradiated form could be accurately calculated, suggesting that chromophore maturation had been impeded on production of the protein in the dark. Live cell imaging by widefield microscopy revealed that PAmCherry^{197azF} could be rapidly activated by UV irradiation, with an observed $t_{1/2}$ at 350 nm of 10 sec (Fig 1d). UV irradiated PAmCherry^{197azF} showed higher apparent photostability than native mCherry, a key characteristic of photoactivatable fluorescent proteins (compare Fig 1f and S2b); no apparent decrease in cellular fluorescence was observed after 60 sec of imaging. More detailed *in vitro* studies demonstrated that on irradiation, fluorescence increased ~14 fold in intensity with a final λ_{EX} and λ_{EM} similar to mCherry (Fig 3a and Table 1). While irradiation resulted in functional activation, presumably through inducing chromophore maturation, the irradiated protein was less bright than native mCherry (Table 1) but could still imaged by microscopy (Fig 1e).

I197 lies just above the plane of the chromophore in mCherry at an equivalent structural position to T203 in GFP (Fig S5). Together with numerous additional mutations, substitution of I197 (to arginine) has previously contributed towards the generation of useful photoactivatable mCherry variants [18]. In contrast to the observations here for PAmCherry^{I197azF}, replacement of T203 in sfGFP with azF did not appear to significantly affect chromophore maturation but did red shift excitation and emission in the dark [13]. The absence here of a red shift in spectral properties suggests that PAmCherry^{197azF} does not display aromatic stacking between residue 197 and the chromophore. Also, photolysis of sfGFP Y203azF results in a major reduction in extinction coefficient (~5 fold)[13] whereas substantial increase is observed for PAmCherry^{I197azF} (Table 1). Thus, in this case the influence of azF and its photochemistry on function is not simply transferred from sfGFP to mCherry highlighting the role played by the local chemical environment.

I197 together with K70 are known to have an important role in chromophore maturation in mCherry[19], especially concerning the Y67 Cα-Cβ oxidation step, with K70 acting as a general base for proton abstraction[20]. Given the proximity of K70 and I197 in space (Fig S5), replacement of residue 197 is likely to disrupt the positioning of K70, so preventing it from acting as a general base. It is now thought that chromophore maturation of DsRed derived proteins (such as mCherry) proceed via a blue emitting intermediate, equivalent to the conjugated imidazolinone and acylimine groups[19,20]. Loss of the potential Cα-Cβ oxidation step does not explain the apparent lack of this intermediate form in the dark state. This suggests that prior to irradiation, chromophore maturation progresses to, at most, the formation of the initial cyclised non-oxidised form (through the linking of residues M66 and G68). One hypothesis is that the phenyl azide group alters the positions of key residues such as K70 involved in chromophore maturation at both the Y67 Cα-Cβ and the M66 N-Cα oxidation steps required for a completed conjugation system. It could be possible that loss of molecular N_2 (and associated local structural rearrangements) together with the formation of the nitrene radical itself and/or a final reaction product (e.g. phenyl amine) is involved in the maturation pathway, substituting for or modulating the role played by residues such as K70 in mCherry. Unfortunately, we were unable to crystallise this variant. It is important to note that it is the azide moiety that is likely to play the key role in controlling maturation in PAmCherry^{197azF} as mutation to tyrosine (I197Y mutant) does not affect mCherry maturation fluorescence (Fig S6).

The mCherry Y67azF variant (equivalent to Y66 in GFP), termed PEmCherry^{67azF} (where PE refers to photoenhancement), has the tyrosine within the chromophore replaced. The transmissive properties of PEmCherry^{67azF} were very different to mCherry with cell lysates turning from a purple to red colour (Fig 1c), with replacement of the phenol group with phenyl azide in the chromophore the likely cause (*vide infra*). PEmCherry^{67azF} was produced as a weakly fluorescent protein with the emission peak blue shifted by ~50 nm compared to mCherry (Table S1), which is in keeping with previous observations that the electron rich azido group can act as a fluorescence quencher[8, 21]. On UV irradiation with low power UV light, a 3.4 fold increase in fluorescence was observed, with the blue shift in λ_{EX} and λ_{EM} compared to mCherry retained (Fig 3b and Table S1). Previous work with GFP suggests that this is caused by the conversion of the phenyl azide to a phenyl amine [14]. Replacing azF at residue 67 with *p*-amino-L-phenylalanine to mimic the potential photochemical endpoint produced a protein with similar maximal excitation and emission wavelengths to that of the irradiated PEmCherry^{67azF} (Fig S7), supporting the idea of conversion to the phenyl amine. The exchange of the phenol, or more accurately phenolate to phenyl amine changes the electron donation strength of the aromatic component and thus the resonant structures of the chromophore. This in turn could cause the observed blue shift in fluorescence.

The genetic incorporation of phenyl azide chemistry into proteins is a potentially general tool for controlling protein activity through the use of light without the need for bulky

protein domains and additional cofactors. As demonstrated here with the widely used autofluorescent protein mCherry, the position within the protein's molecular structure is critical to how the potential photochemical pathway taken will ultimately impact function. Through incorporation of a single ncAA at three disparate positions in the protein core, we have generated PD, PA and PE mCherry variants, that could be developed into useful tools for microscopy. FRAP (fluorescence recovery after photobleaching) microscopy [22] is normally hindered by the photostability of autofluorescent proteins meaning long and relatively intense illumination are required to deactivate the protein. This results in the loss of temporal resolution. PDmCherry^{143azF} is relatively photostable at imaging wavelengths but can be rapidly deactivated at low light energy making it potentially an excellent probe for furthering FRAP microscopy. PALM (photoactivated localisation microscopy) requires photoactivatable fluorescent proteins with high levels of photostability [23, 24], a characteristic we have successfully introduced into PAmCherry^{197azF}. While photocontrol of autofluorescent proteins (including mCherry [18]) require multiple canonical mutations to achieve useful light-sensitive properties, we have shown here that incorporation of a single light sensitive ncAA can achieve a similar endpoint and sample different photochemical effects. Improved approaches for efficient and higher yielding ncAAs containing proteins in different cells and organisms [25] combined with the inherent chemical genetic element (ncAA-dependent protein production) will broaden the potential use with regards to autofluorescent proteins and proteins in general.

Notes and references

[a] School of Biosciences, Cardiff University, Cardiff, UK

[b] School of Medicine, Cardiff University, Cardiff, UK.

* Correspondence: D. Dafydd Jones. School of Biosciences, Cardiff University, Cardiff, UK. Tel: 02920 20874290; E-mail: jonesdd@cardiff.ac.uk.

† The PDB accession codes for dark and irradiated PDmCherry^{143azF} are 4ZIN and 4ZIO. We would like to thank the staff at the Diamond Light Source for the supply of facilities and beam time, especially Beamline I03 and I04 staff. We thank BBSRC (BB/H003746/1 and BB/ M000249/1), EPSRC (EP/J015318/1) and Cardiff SynBio Initiative/SynBioCite for supporting this work.

Electronic Supplementary Information (ESI) available: Detailed methods, Supporting Figs S1-S7, Supporting Tables S1-S3. See DOI: 10.1039/c000000x/

1. K. Deisseroth, *Nat Methods*, 2011, **8**, 26-29.
2. A. Gautier, C. Gauron, M. Volovitch, D. Bensimon, L. Jullien and S. Vriz, *Nat Chem Biol*, 2014, **10**, 533-541.
3. J. E. Toettcher, C. A. Voigt, O. D. Weiner and W. A. Lim, *Nat Methods*, 2011, **8**, 35-38.
4. A. Moglich and K. Moffat, *Photochemical & photobiological sciences*, 2010, **9**, 1286-1300.
5. A. Gautier, A. Deiters and J. W. Chin, *J Am Chem Soc*, 2011, **133**, 2124-2127.
6. J. Chin, S. Santoro, A. Martin, D. King, L. Wang and P. Schultz, *J Am Chem Soc*, 2002, **124**, 9026-9027.
7. S. Reddington, P. Watson, P. Rizkallah, E. Tippmann and D. D. Jones, *Biochem Soc Trans*, 2013, **41**, 1177-1182.
8. J. L. Morris, S. C. Reddington, D. M. Murphy, D. D. Jones, J. A. Platts and E. M. Tippmann, *Organic Letters*, 2013, **15**, 728-731.
9. A. Miyawaki, D. M. Shcherbakova and V. V. Verkhusha, *Curr Opin Struc Biol*, 2012, **22**, 679-688.
10. R. Y. Tsien, *Annual review of biochemistry*, 1998, **67**, 509-544.
11. D. M. Shcherbakova and V. V. Verkhusha, *Curr Opin Chem Biol*, 2014, **20**, 60-68.
12. W. Niu and J. Guo, *Mol Biosyst*, 2013, **9**, 2961-2970.
13. S. C. Reddington, A. J. Baldwin, R. Thompson, A. Brancale, E. M. Tippmann and D. D. Jones, *Chemical Science*, 2015, **6**, 1159-1166.
14. S. C. Reddington, P. J. Rizkallah, P. D. Watson, R. Pearson, E. M. Tippmann and D. D. Jones, *Angewandte Chemie Int Ed*, 2013, **52**, 5974-5977.
15. N. C. Shaner, R. E. Campbell, P. A. Steinbach, B. N. Giepmans, A. E. Palmer and R. Y. Tsien, *Nat Biotech*, 2004, **22**, 1567-1572.
16. X. Shu, N. C. Shaner, C. A. Yarbrough, R. Y. Tsien and S. J. Remington, *Biochemistry*, 2006, **45**, 9639-9647.
17. J. D. Pedelacq, S. Cabantous, T. Tran, T. C. Terwilliger and G. S. Waldo, *Nat Biotech*, 2006, **24**, 79-88.
18. F. V. Subach, G. H. Patterson, S. Manley, J. M. Gillette, J. Lippincott-Schwartz and V. V. Verkhusha, *Nat Methods*, 2009, **6**, 153-159.
19. F. V. Subach, V. N. Malashkevich, W. D. Zencheck, H. Xiao, G. S. Filonov, S. C. Almo and V. V. Verkhusha, *Proc Natl Acad Sci USA*, 2009, **106**, 21097-21102.
20. F. V. Subach and V. V. Verkhusha, *Chem Rev*, 2012, **112**, 4308-4327.
21. K. Sivakumar, F. Xie, B. M. Cash, S. Long, H. N. Barnhill and Q. Wang, *Organic letters*, 2004, **6**, 4603-4606.
22. A. Miyawaki, *Nature biotechnology*, 2004, **22**, 1374-1376.
23. M. Fernandez-Suarez and A. Y. Ting, *Nat Rev Mol Cell Biol*, 2008, **9**, 929-943.
24. J. Lippincott-Schwartz and G. H. Patterson, *Trends Cell Biol*, 2009, **19**, 555-565.
25. J. W. Chin, *Ann Review Biochem*, 2014, **83**, 379-408.

